



## UvA-DARE (Digital Academic Repository)

### Neutron-inelastic-scattering study of the compound YbCuAl

Murani, A.P.; Mattens, W.C.M.; de Boer, F.R.

**DOI**

[10.1103/PhysRevB.31.52](https://doi.org/10.1103/PhysRevB.31.52)

**Publication date**

1985

**Published in**

Physical Review. B, Condensed Matter

[Link to publication](#)

**Citation for published version (APA):**

Murani, A. P., Mattens, W. C. M., & de Boer, F. R. (1985). Neutron-inelastic-scattering study of the compound YbCuAl. *Physical Review. B, Condensed Matter*, 31(1), 52-58.  
<https://doi.org/10.1103/PhysRevB.31.52>

**General rights**

It is not permitted to download or to forward/distribute the text or part of it without the consent of the author(s) and/or copyright holder(s), other than for strictly personal, individual use, unless the work is under an open content license (like Creative Commons).

**Disclaimer/Complaints regulations**

If you believe that digital publication of certain material infringes any of your rights or (privacy) interests, please let the Library know, stating your reasons. In case of a legitimate complaint, the Library will make the material inaccessible and/or remove it from the website. Please Ask the Library: <https://uba.uva.nl/en/contact>, or a letter to: Library of the University of Amsterdam, Secretariat, Singel 425, 1012 WP Amsterdam, The Netherlands. You will be contacted as soon as possible.

## Neutron-inelastic-scattering study of the compound YbCuAl

A. P. Murani

*Institut Laue-Langevin, 156X, 38042 Grenoble, France*

W. C. M. Mattens and F. R. de Boer

*Natuurkundig Laboratorium, University of Amsterdam, Valckenierstraat 65, 1018 XE Amsterdam*

G. H. Lander

*Argonne National Laboratory, Argonne, Illinois, 60439\* and Institut Laue-Langevin, 156X, 38042 Grenoble, France*

(Received 26 May 1983; revised manuscript received 29 May 1984)

Neutron-inelastic-scattering measurements on the compound YbCuAl reveal well-defined inelastic-scattering magnetic-response peaks superposed over a broad quasielastic-scattering spectrum at low temperatures. The inelastic-scattering peaks disappear around the temperature at which the maximum in the static susceptibility occurs ( $\sim 30$  K), above which the full spectral response can be described by a single quasielastic-scattering Lorentzian spectrum. The quasielastic-scattering spectral width increases again below 30 K, following the same trend as the spin fluctuation rate  $\tau_{\text{eff}}^{-1}$  obtained from NMR measurements.

## INTRODUCTION

Many rare-earth alloys and compounds, particularly those of Ce and Yb, often show anomalous physical properties accompanied occasionally by significant volume anomalies, which are attributed to intermediate-valence, or valence-fluctuation, phenomena.<sup>1</sup> We report neutron-inelastic-scattering measurements of the magnetic spectral response of one such compound—namely YbCuAl—between 5 K and room temperature. Although the lattice parameters of YbCuAl (Ref. 2) suggest a valence close to 3 and the  $L_{\text{III}}$  absorption-edge spectra<sup>3</sup> indicate a similar result (2.95), nevertheless there are marked anomalies in several physical properties. Its magnetic susceptibility,<sup>4</sup> which shows a broad maximum around 30 K, and the specific heat, with its enhanced magnitude of the electronic specific heat coefficient  $\gamma = 260$  mJ/K<sup>2</sup> mol, are generally thought typical of mixed-valence systems, undergoing a possible transition to the Fermi-liquid state at low temperatures.<sup>5</sup> Further evidence for the change in the nature of magnetic state at low temperatures is provided by the NMR Knight-shift data,<sup>6</sup> which show that below the temperature of the maximum in the susceptibility the Knight shift deviates from its linear dependence on the susceptibility.

The present results were first presented in 1980.<sup>7</sup> At that time we realized that additional inelastic, or possibly crystal-field, transitions were present in the data. However, they appeared to coincide in energy with a sharp maximum in the phonon density of states. Since the experiment measures both functions—both the nuclear and magnetic response—this led to the necessity of developing very careful subtraction procedures before assigning inelastic-scattering peaks to the magnetic-response spectrum. These have now been developed and are reported in this paper. An additional complication is that Yb has one of the largest nuclear cross sections ( $\sigma_{\text{scatt}} = 25$  b) of any

metal in the Periodic Table, so that simulating the phonon scattering by using a nonmagnetic “control material” (in our case <sup>39</sup>Y, with  $\sigma_{\text{scatt}} = 7.7$  b) is not a totally valid procedure.

In the present paper we present a detailed analysis of this data with a careful phonon subtraction procedure which permits us to identify well-defined magnetic inelastic-scattering peaks superposed at a broad quasielastic-scattering spectrum at low temperatures (5 K). These inelastic-scattering peaks, however, disappear at a temperature close to that at which the maximum in the static susceptibility occurs ( $\sim 30$  K).

## EXPERIMENTAL

The neutron-inelastic-scattering measurements were made on the time-of-flight spectrometer IN4 at the Institut Laue-Langevin using neutrons of incident energy 12.6 and 50.7 meV. Detectors covered the angular ranges  $9^\circ$  to  $70^\circ$  and also  $150^\circ$  to  $160^\circ$ ; low-angle detectors permit us to measure both the magnetic and the phonon contributions whereas the group of counters at high angles detect almost purely the phonon contribution, since for the short-wavelength neutrons ( $\lambda_i = 1.27$  Å,  $E_i = 50.7$  meV) these high scattering angles correspond to rather large  $Q$  values where (the square of) the  $4f$  magnetic form factor and hence the magnetic scattering is negligibly small. Measurements were also made on the isostructural nonmagnetic YCuAl to study the energy and  $Q$  dependence of the phonons, which provides an important check on the analysis. The relative efficiencies of the detectors were calibrated by measurement on a standard vanadium sample, and background scattering was determined by measurements on the empty sample holder and a cadmium plate replacing the sample. The detectors were grouped over angular ranges of  $9^\circ$  in order to increase the statisti-

cal accuracy of the data. In conversion from the time-of-flight to the energy scale, corrections for the wavelength-dependent transmission, i.e., self-shielding, were also applied. After subtraction of the phonons, using the procedures described below, the resultant magnetic-response spectrum was corrected for the  $Q$  variation of intensity as a function of energy transfer for fixed scattering angles  $2\theta$  using the  $\text{Yb}^{3+}$  form-factor dependence.<sup>8</sup>

The large ( $\sim 50$  g) sample of YbCuAl used in the neutron scattering experiment was a composite of several smaller samples prepared under identical conditions by melting together in outgassed molybdenum crucibles appropriate amounts of pure metals: Yb (of 99.9% purity from Koch-light Laboratories Ltd.) and Al and Cu (of 99.995% and 99.999% purity, respectively, from Johnson Matthey and Co.). The crucibles were sealed by arc melting under argon atmosphere and subsequently heated in an induction furnace for 30 min at 1300°C. During this process the crucibles were reversed a few times in order to ensure good mixing of the constituents and then quenched into water. The samples were finally annealed at 830°C for one week. X-ray diffraction patterns taken on small grains of different ingots revealed the characteristic pattern for the hexagonal  $\text{Fe}_2\text{P}$ -type structure and no second phase. This lattice parameter agrees within experimental accuracy with the value given by Dwight *et al.*<sup>2</sup> The reproducibility of sample quality was extremely good as verified by bulk susceptibility measurements on the various samples.

The YCuAl sample was prepared by arc melting the constituent elements placed on a water-cooled copper hearth under argon atmosphere. The resulting buttons were annealed at 800°C. No second phase could be detected in the x-ray patterns of these samples.

## RESULTS AND ANALYSIS

The time-of-flight spectra measured with the use of 50.7-meV neutrons were converted to the spectral response  $S(Q, \omega)$ . The results are shown in Fig. 1. Since the measurements are made at fixed scattering angles  $2\theta$ , each data point represents a different set of  $Q$  and  $\omega$  values. As mentioned earlier, the data at the highest scattering angle,  $2\theta=154^\circ$ , corresponding to an elastic  $Q_0=9.6 \text{ \AA}^{-1}$ , contain phonon scattering since the magnetic contribution is negligibly small at these high  $Q$  values. In Fig. 2 we show corresponding data obtained for the nonmagnetic YCuAl sample, which represents purely phonon scattering. We note that since the incident neutron wavelength is small and the samples polycrystalline, the observed scattering is averaged over several Brillouin zones. Because of the different atomic masses of  $^{39}\text{Y}$  and  $^{70}\text{Yb}$ , the phonon "peaks" occur at different energies in the two compounds. Furthermore, the scattering cross sections of Y and Yb are quite different [ $\sigma(^{39}\text{Y})=7.7 \text{ b}$ ,  $\sigma(^{70}\text{Yb})=25 \text{ b}$ ], so that the phonon spectra measured for YCuAl cannot be directly used to correct for phonon scattering in the magnetic sample. Consequently we have followed a procedure in which we study the angular dependence of the phonons in YCuAl and obtain a scaling function  $C_\theta^\theta(\omega)$  between a pair of high- and

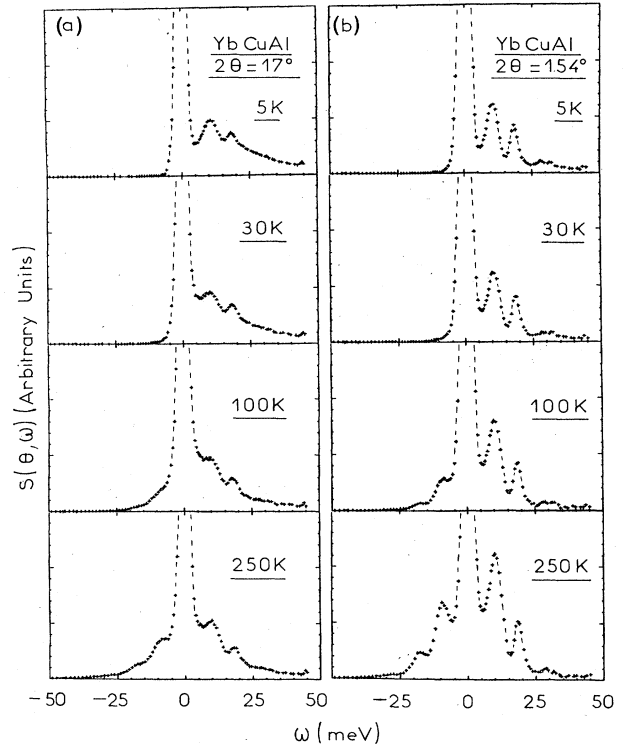


FIG. 1. Spectral response  $S(\theta, \omega)$  for YbCuAl as a function of energy transfer  $\omega$  for two fixed scattering angles (a)  $2\theta=17^\circ$  and (b)  $2\theta=154^\circ$ . The low-angle spectra contain both magnetic and phonon-scattering contributions while the high-angle spectra represents almost purely phonon scattering.

low-angle spectra, and use it (with small modifications) to correct for phonons in YbCuAl. This analysis was not performed in Ref. 7 and is therefore new. We have proceeded to obtain a scaling function  $C_\theta^\theta(\omega)$  between the

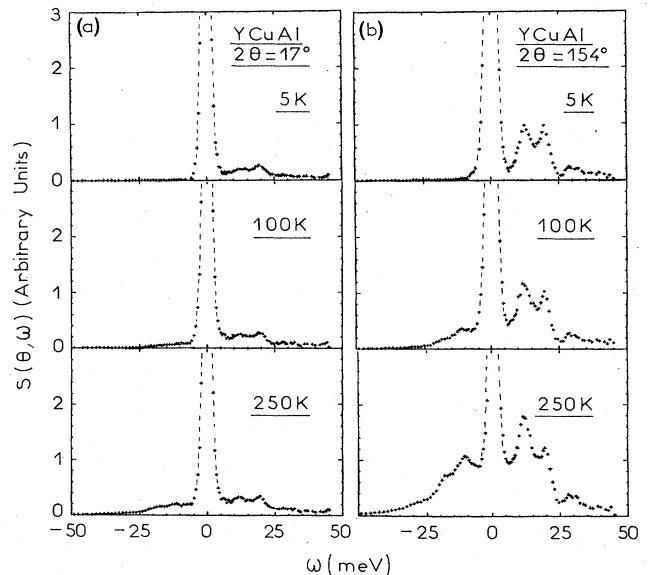


FIG. 2. Spectral response  $S(\theta, \omega)$  for the nonmagnetic YCuAl sample as function of energy transfer  $\omega$  for two fixed scattering angles (a)  $2\theta=17^\circ$  and (b)  $2\theta=154^\circ$ .

high- and low-angle spectra such that  $S_{\text{ph}}(\theta, \omega) = C_{\theta}^{\text{ph}}(\omega) S_{\text{ph}}(\theta', \omega)$  (within the limits of the statistical accuracy of the data). Such a function is not difficult to obtain for the YCuAl sample since it is simply the ratio  $S(\theta, \omega)/S(\theta', \omega)$ . We should note the  $C_{\theta}^{\text{ph}}(\omega)$  is somewhat energy dependent, varying by  $\sim 25\%$  across the energy transfer of interest, because for different values of  $\theta$  there is a different sampling of the phonon density of states. This resultant function was smoothed and applied to YbCuAl but still was found to leave some inelastic "structure" even in the high-temperature data presumably because the phonon peaks do not occur at exactly the same energies in the two cases, and because of the much larger coherent cross section of Yb. Later we will show that the magnetic scattering at both 100 and 250 K is almost certainly a smooth Lorentzian function so that to obtain final values of  $C_{\theta}^{\text{ph}}(\omega)$  we have *assumed* that the 100 K data consists, at low  $Q$ , of a smooth magnetic part and that any structure at low  $Q$  arises from the phonon contribution. The resultant  $C_{\theta}^{\text{ph}}(\omega)$  function is similar to that obtained from YCuAl in its form. This function has then been used *without modification* to correct for phonon scattering at all temperatures.  $C_{\theta}^{\text{ph}}(\omega)$  is not, therefore, temperature dependent, although, again because of the sampling in the various Brillouin zones and the changing phonon populations, one might expect some small changes.

The resultant spectra are presented as  $\chi''(\theta, \omega)$  in Fig. 3(b), which has the merit that the Bose-Einstein factor  $[n(\omega) + 1]$  is eliminated, making the comparison among various temperatures much more direct. As expected, the high-temperature data at 250 K yield a broad quasielastic-scattering response and even the data at 30 K can be adequately represented by a single quasielastic-scattering Lorentzian spectrum. At 5 K however, significant peaks are left over in the resultant spectrum.

The neutron scattering cross section for a paramagnetic system may be expressed as<sup>9</sup>

$$\frac{d^2\sigma}{d\Omega d\omega} = N \left[ \frac{\gamma e^2}{mc^2} \right]^2 \frac{k'}{k_0} S(Q, \omega), \quad (1)$$

with

$$S(Q, \omega) = \frac{2}{\pi} [n(\omega) + 1] \chi''_{\text{av}}(Q, \omega), \quad (2)$$

where  $N$  is the number of spins;  $(\gamma e^2/mc^2)^2$ , the coupling constant between the neutron and the magnetic moment;  $k_0$  and  $k'$ , the ingoing and outgoing neutron wave vectors; and  $S(Q, \omega)$ , the scattering function, which is proportional to the imaginary part of the susceptibility response  $\chi''_{\text{av}}(Q, \omega)$  via the population factor

$$[n(\omega) + 1] = [1 - \exp(-\omega/T)]^{-1}.$$

The subscript av denotes that susceptibility response is averaged over the three components  $\chi_{xx}, \chi_{yy}, \chi_{zz}$ , which are, of course, equal for an isotropic system. Under this assumption the subscript is henceforth dropped for convenience. We recall that phonon scattering may also be represented in a manner analogous to Eq. (1) with

$$S_{\text{ph}}(Q, \omega) = [n(\omega) + 1] g(Q, \omega). \quad (3)$$

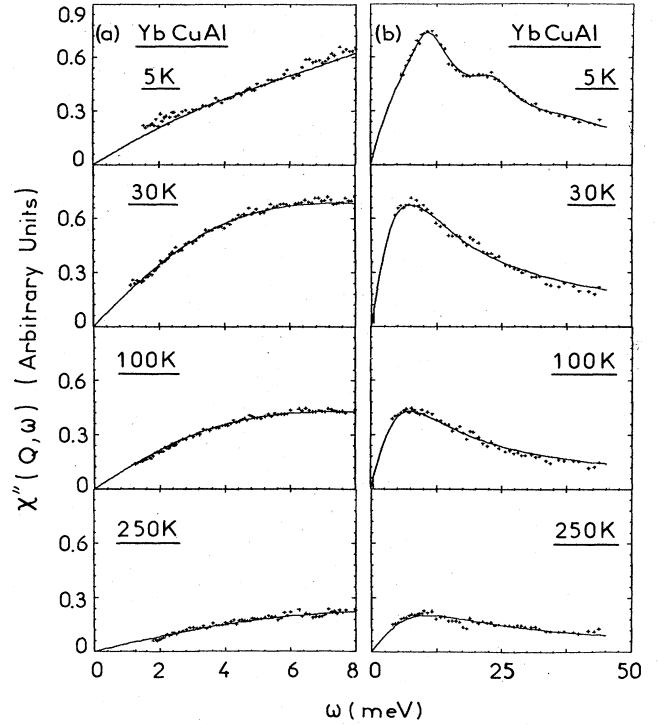


FIG. 3. Imaginary part of the magnetic susceptibility response  $\chi''(Q, \omega)$  obtained after the full phonon correction procedure described in the text. (a) Data obtained with neutrons of incident energy  $E_i = 12.6$  meV and (b) data obtained with  $E_i = 50.7$  meV. The solid lines through the data points represent fits discussed in the text. The same parameters apply in both cases.

However, unlike  $\chi''(Q, \omega)$  which is, in general, temperature dependent, the function  $g(Q, \omega)$  is not strongly dependent on temperature. In the present measurements this is closely borne out up to  $\sim 100$  K for both YCuAl and YbCuAl samples. At higher temperatures, however, thermal broadening and multiphonon processes modify the spectral response noticeably as seen from the 250 K spectra.

The observed constancy of  $g(Q, \omega)$  up to about 100 K suggests a second independent method to ascertain the evolution of magnetic structure in the spectral response at low temperatures. In the case where both magnetic and phonon scattering are present, Eqs. (2) and (3) can be combined to give

$$S(Q, \omega)[n(\omega) + 1]^{-1} = \frac{2}{\pi} \chi''(Q, \omega, T) + g(Q, \omega), \quad (4)$$

where the variable  $T$  is included explicitly to emphasize the  $T$  dependence of  $\chi''(Q, \omega)$ . Since  $g(Q, \omega)$  is found to be temperature independent up to 100 K, a simple subtraction of the scattering functions normalized to their population factors, yields the difference between  $\chi''(Q, \omega)$  at the two temperatures. We have evaluated these differences for the 5- and 30-K spectra relative to the 100-K data. The results for the low-angle spectra are shown in Fig. 4. As expected, the high-angle-difference spectra

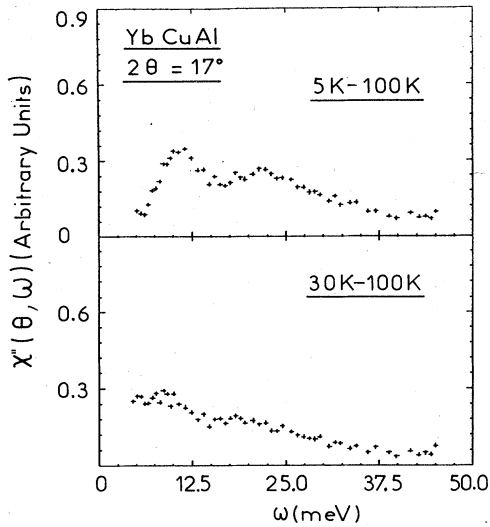


FIG. 4. Difference spectra  $\chi''(\theta, \omega)$  for YbCuAl relative to the 100 K spectrum at  $2\theta = 17^\circ$ , for two temperatures, 5 and 30 K. We note that since the phonon contribution expressed as  $g(\theta, \omega)$  is almost identical at all three temperatures, it is subtracted out exactly in the difference spectra which therefore represents a purely magnetic contribution above that in the 100 K spectrum. Similar differences for the high-angle spectra yield fluctuations about an overall zero residue.

give fluctuations of about a zero residue for both temperatures, whereas the low-angle spectra at 5 K show well-defined inelastic-scattering peaks (superposed over a broad quasielastic-scattering response which almost subtracts out). At temperatures as high as 30 K, however, the inelastic-scattering structure has almost completely disappeared.

As discussed below, the origin of the inelastic-scattering peaks is not entirely clear. We believe, however that their magnetic character is demonstrated beyond reasonable doubt. Hence, we express the imaginary part of the susceptibility response in terms of quasielastic-scattering and several inelastic-scattering magnetic peaks as

$$\chi''(Q, \omega) = F^2(Q)\omega \left[ A_0 f_0(\omega) + \sum_i A_i f_i(\omega + \omega_i) \right], \quad (5)$$

where  $F(Q)$  is the magnetic form factor,  $A_0, A_i$  are the temperature- and  $Q$ -dependent amplitudes, and  $f_0, f_i$  are the quasielastic-scattering and inelastic-scattering spectral functions, respectively. We assume that the functions  $f_0, f_i$  are Lorentzian, i.e.,

$$f_0(\omega) = [\omega^2 + \Gamma_0^2(T)]^{-1}, \quad (6)$$

and

$$f_i(\omega \pm \omega_i) = [(\omega - \omega_i)^2 + \Gamma_i^2(T)]^{-1} + [(\omega + \omega_i)^2 + \Gamma_i^2(T)]^{-1}, \quad (7)$$

where  $\Gamma_0(T)$  and  $\Gamma_i(T)$  are temperature-dependent half-widths. In general,  $\omega_i$  could also be temperature dependent. Hence, using the Kramers-Kronig relation we have

$$\chi'(Q) = F^2(Q) \left[ A_0(T)\Gamma_0^{-1}(T) + 2 \sum_i A_i(T)\Gamma_i^{-1}(T) \right], \quad (8)$$

where we have assumed throughout that any  $Q$  dependence of  $\chi$  is via the form factor only. The fitted parameters must therefore cross check for a correct prediction of the static susceptibility.

We have attempted to fit the phonon-corrected spectra shown in Fig. 3 to the above form of the magnetic response function [Eq. (5)]. In order to achieve unambiguous fits especially at 5 and 30 K, the low-energy data obtained with 12.6-meV neutrons were particularly useful since they provide data resolved from the incoherent elastic signal closer to zero energy and therefore help to fix the initial part of the curve. We should mention that in measurements with the 12.6-meV neutrons the "trajectory" followed through the  $Q$ - $\omega$  plane and hence the phonon sampling is quite different from that with the higher-energy neutrons. Few phonon branches are cut so that the scattering is principally dominated by incoherent phonon processes which are found to be only  $\sim 3\%$  of the signal in YbCuAl at low angles. In making this small correction we have used the YCuAl spectrum, suitably scaled with the nuclear cross sections. The results are given in Fig. 3(a).

The results of the fits of Eq. (5) to the curves in Fig. 3 are given in Table I and are the solid lines in Fig. 3. For the 5-K data, the best fits are with two inelastic-scattering lines centered at  $10.0 \pm 0.5$  and  $23 \pm 1$  meV. Even after this fit a small amount of inelastic scattering remained for  $E > 30$  meV, but we are unable to claim unambiguously that there is a third inelastic peak. For the 30-K data the fit with or without an inelastic-scattering structure is equally good and we have shown in Fig. 3 the fit corresponding to the simple Lorentzian. This is also evident from Fig. 4. Note that in Figs. 3(a) and 3(b) the *same* fit parameters produce the solid lines through the data taken with the two different incident energies.

In Fig. 5 the static susceptibility  $\chi(Q)$  obtained from the resultant parameters of the fits using Eq. (8) is plotted as a function of temperature together with the continuous curve representing the bulk susceptibility  $\chi$  reported earlier.<sup>4</sup> The neutron data were scaled to the bulk susceptibility (relative to the 100-K point) since no attempt was made to put them on an absolute scale independently. The close agreement between the temperature dependence of the two measurements suggests single-ion character of the spectral response.

In Fig. 6 the quasielastic-scattering linewidth is plotted as a function of temperature (solid circles). In the same diagram we have included the inverse spin-correlation times  $\tau_{\text{eff}}^{-1}$  determined from NMR measurements.<sup>6</sup> Assuming that the susceptibility response is independent of the scattering vector  $Q$  and is isotropic, i.e.,  $\chi_{xx} = \chi_{yy} = \chi_{zz}$ , the spin-correlation time is given by<sup>10</sup>

$$\tau_{\text{eff}} = \left[ \frac{\sum_Q [H_{\text{hf}}(Q)]^2}{(H_{\text{hf}}^0)^2} \right] \frac{\chi''(\omega_n)}{\omega_n \chi}. \quad (9)$$

where the magnitude of the quantity inside the large parentheses is determined by the form of the hyperfine coupling between the nucleus and the conduction electrons, and is unity for localized coupling.  $\omega_n$  is the NMR frequency which is  $\sim 10^{-4}$  meV, i.e., sensibly zero on the

TABLE I. Summary of the resultant parameters of the fits to the phonon corrected spectra shown in Fig. 5. The errors in the amplitudes  $A_0, A_i$  are coupled to those in the widths.

| $T$<br>(K) | $A_0$ | $\Gamma_0$<br>(meV) | $A_1$ | $\omega_1$<br>(meV) | $\Gamma_1$<br>(meV) | $A_2$ | $\omega_2$<br>(meV) | $\Gamma_2$<br>(meV) |
|------------|-------|---------------------|-------|---------------------|---------------------|-------|---------------------|---------------------|
| 5          | 5.73  | 7.5<br>$\pm 0.5$    | 0.53  | 10.0<br>$\pm 0.5$   | 3.6<br>$\pm 0.5$    | 0.14  | 23<br>$\pm 1$       | 4.2<br>$\pm 0.5$    |
| 30         | 8.38  | 6.5<br>$\pm 0.5$    | 0.13  | 10.0<br>$\pm 1$     | 5.4                 |       |                     |                     |
|            | 9.64  | 7.0<br>$\pm 0.5$    | 0     |                     |                     |       |                     |                     |
| 100        | 6.01  | 7.0<br>$\pm 0.5$    | 0     |                     |                     |       |                     |                     |
| 250        | 3.94  | 9.6<br>$\pm 0.8$    | 0     |                     |                     |       |                     |                     |

scale of the present data. Hence we write

$$\tau_{\text{eff}} = H \lim_{\omega \rightarrow 0} \frac{\chi''(\omega)}{\omega \chi}, \quad (10)$$

where  $H$  represents the proportionality constant within the large parentheses in (9).

The quantity  $\tau_{\text{eff}}$  can be easily determined from the present measurements, since from Eqs. (5) to (8) we obtain

$$\tau_{\text{eff}} = H \frac{A_0 \Gamma_0^{-2} + 2 \sum_i A_i [(\Gamma_i^2 + \omega_i^2)^{-1}]}{A_0 \Gamma_0^{-1} + 2 \sum_i A_i \Gamma_i^{-1}}. \quad (11)$$

If the spin dynamics could be represented by a quasielastic-scattering spectra function, i.e., if all  $A_i = 0$  (for  $i \neq 0$ ) then

$$\tau_{\text{eff}}^{-1} = \Gamma_0, \quad (12)$$

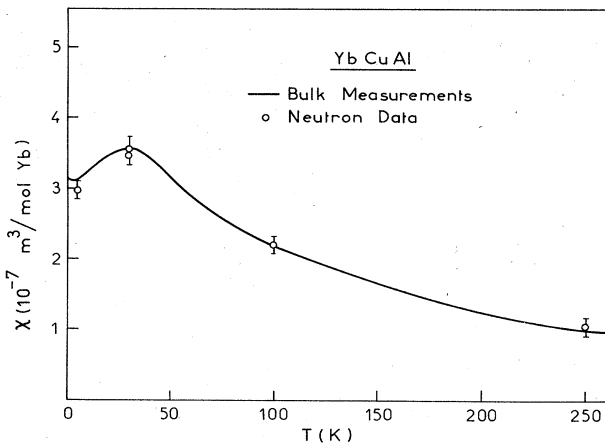


FIG. 5. Static susceptibility  $\chi$  for YbCuAl. The continuous curve gives the bulk susceptibility reported earlier (Ref. 4). The open symbols represent the susceptibility  $\chi(Q)$  obtained from the present neutron spectra, using Eq. (8) and the fitted parameters. The data have been scaled to the bulk measurements relative to the 100-K point.

where the "coupling constant"  $H$  is assumed unity for localized coupling. Thus at high temperatures, where the spin dynamics is purely relaxational, we expect a one-to-one correspondence between  $\tau_{\text{eff}}^{-1}$  and the measured quasielastic-scattering spectral width  $\Gamma_0$ . However, at low temperatures when the inelastic-scattering features appear in the spectral response the  $\tau_{\text{eff}}^{-1}$  evaluated from the neutron data shown by the triangles deviates significantly from  $\Gamma_0$ . The close agreement between the neutron and the NMR data is remarkable in view of the assumptions about the form of the hyperfine coupling (localized) and isotropy of the spectral response.

## DISCUSSION

The observation of inelastic-scattering magnetic peaks at low temperature and their rapid disappearance at higher temperatures around the temperature at which the maximum in the static susceptibility occurs represents the dominant feature of the present results.

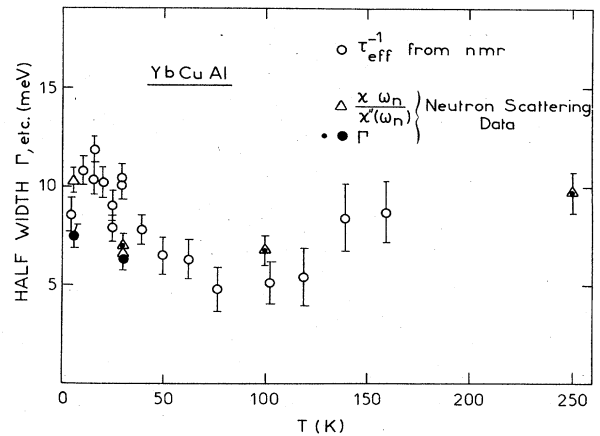


FIG. 6. Temperature dependence of the quasielastic-scattering spectral width  $\Gamma$  (solid points), the quantity  $\chi\omega_n/\chi''(\omega_n)$  (triangles), and the spin-fluctuation rate  $\tau_{\text{eff}}^{-1}$  (open circles) from NMR measurements (Ref. 6).

For a simple crystal-field model with the  $\text{Yb}^{3+}$  ion in a present crystal structure we would expect four doublets. At 5 K, only the ground state would be populated so that at most three crystal-field transitions would be expected. If the energy of the first is  $10.0 \pm 0.5$  meV ( $\omega_1$  in Table I), then the overall splitting would be about 40 meV ( $\sim 500$  K), which is much larger than normal Yb systems. Even more important, if we increase the temperature to 30 K ( $\sim 2.5$  meV), the population of the states would *not* be expected to vary so that the ground to first excited-state intensity should stay constant to within 10%. Instead  $A_1$  in Table I decreases by a factor of at least 4 (from 0.53 to 0.13) on warming from 5 to 30 K. This essentially precludes the possibility that these inelastic-scattering peaks are *simple* crystal-field transitions.

We may then consider more complex forms of crystal-field excitations, such as those treated by Becker *et al.*<sup>11</sup> for  $\text{Ce}^{3+}$  ions in a cubic crystal field. These authors show how the inclusion of a coupling between the  $4f$  moment and conduction electrons modifies the simple crystal-field description. Their results show broad quasielastic-scattering and inelastic-scattering peaks at finite temperatures. With increasing temperature the spectral weight from the inelastic-scattering peak is transferred progressively to the quasielastic-scattering part until above some temperature only a broad quasielastic-scattering remains. Such behavior is clearly seen for example in the Kondo system  $\text{CeInAg}_2$  which orders antiferromagnetically at  $T_N = 2.2$  K.<sup>12</sup>

The analogy between the predictions of the theory of Becker *et al.*<sup>11</sup> and observations in YbCuAl breakdown at low temperatures. According to the theory the quasielastic-scattering linewidth should vary linearly with temperature (Korringa law) and hence tend to zero at absolute zero which is consistent with conservation of magnetic moment and the Curie term in the susceptibility. In YbCuAl, however, we observe broad quasielastic scattering of finite width and intensity as  $T \rightarrow 0$  K, suggesting progressive demagnetization as  $T \rightarrow 0$  K. At present we are unaware of any theory which treats crystal-field effects in the latter situation.

The present results may be compared with observations in related systems. A close example is that of  $\text{YbCuSi}_2$  which is also considered an intermediate-valence system.<sup>13</sup> In contrast to YbCuAl, however, well-defined crystal-field excitations are thought to be observed at all temperatures up to 300 K, and the spectra have been analyzed in terms of a tetragonal crystal-field scheme.<sup>13</sup>

Crystal-field-like excitations have also been observed in the alloy system  $(\text{Ce}_{1-x}\text{La}_x)_{0.9}\text{Th}_{0.1}$  (Ref. 14) where increasing La concentration stabilizes the valence fluctuations (inferred from the decreasing quasielastic-scattering linewidth  $\Gamma$ ) until a crystal-field-like peak is observed in alloys with La concentration greater than 0.14. In con-

trast to the present case, the inelastic peak in  $(\text{Ce}_{1-x}\text{La}_x)_{0.9}\text{Th}_{0.1}$  remains observable well above the temperature at which the maximum in the susceptibility occurs, and its width is (or assumed to be) comparable with the quasielastic-scattering line width at all temperatures. In YbCuAl, however, the two lower-energy inelastic-scattering peaks are narrower than the quasielastic-scattering linewidth at 5 K. With increasing temperature they apparently broaden and decrease in intensity until by about 30 K, i.e., the temperature of the maximum in the susceptibility, they have disappeared. A second difference with the results in  $(\text{Ce}_{1-x}\text{La}_x)_{0.9}\text{Th}_{0.1}$  alloys is that whereas in the latter alloys the inelastic peak appears only when the quasielastic-scattering width  $\Gamma$  is reduced sufficiently by addition of La, the appearance of inelastic-scattering peaks in YbCuAl is purely a low-temperature phenomenon. Thus, the inelastic-scattering peaks have almost completely disappeared by 30 K although the quasielastic-scattering linewidth is actually smaller there than at 5 K.

## CONCLUSION

We have demonstrated the presence of (at least two) well-defined magnetic inelastic-scattering peaks superposed over a broad quasielastic-scattering spectrum at low temperatures in YbCuAl. The energies of these two inelastic-scattering peaks are very close to the peaks in the phonon spectra. The major part of this paper is concerned with demonstrating that these are indeed magnetic in origin. There is no theoretical reason why such peaks should coincide in energy with peaks in the vibrational density of states and we believe it to be coincidental. At higher temperatures, i.e., above the maximum in the static susceptibility, the inelastic-scattering structure disappears almost completely. This observation correlates strongly with the observed departure around the same temperature from a linear dependence of the NMR Knight shift with the bulk susceptibility in YbCuAl.<sup>6</sup> Similar observations of the appearance of an inelastic-scattering structure below the temperature of the maximum in static susceptibility and its close correlation with the NMR Knight shift anomaly have also been made in the compound  $\text{CeSn}_3$ .<sup>15</sup> Further theoretical input is needed however to appreciate the exact significance of the present results and particularly to understand the origin of the inelastic-scattering peaks.

## ACKNOWLEDGMENT

The work performed at Argonne National Laboratory is supported by the U.S. Department of Energy (Office of Basic Energy Sciences).

\*Present address.

<sup>1</sup>C. M. Varma, Rev. Mod. Phys. 48, 219 (1976); J. M. Lawrence, P. S. Riseborough, and R. D. Parks, Rep. Prog. Phys. 44, 1 (1981).

<sup>2</sup>A. E. Dwight, M. H. Mueller, R. A. Conner, Jr., J. W. Downey, and H. Knott, Trans. Metall. Soc. AIME 242, 2075

(1968).

<sup>3</sup>K. R. Bauschpiess, W. Boksich, E. Holland-Moritz, H. Launois, R. Pott, and D. Wohlleben, in *Valence Fluctuations in Solids*, edited by L. M. Falicov, W. Hanke, and M. B. Maple (North-Holland, Amsterdam, 1981), p. 417.

<sup>4</sup>W. C. M. Mattens, R. A. Elenbaas, and F. R. de Boer, Com-

- mun. Phys. 2, 147 (1977).
- <sup>5</sup>D. M. Newns and A. C. Hewson, J. Phys. F 10, 2429 (1980); M. T. Béal-Monod and J. M. Lawrence, Phys. Rev. B 21, 5400 (1980).
- <sup>6</sup>D. E. MacLaughlin, F. R. de Boer, J. Bijvoet, P. F. de Chatel, and W. C. M. Mattens, J. Appl. Phys. 50, 2094 (1979).
- <sup>7</sup>W. C. M. Mattens, F. R. de Boer, A. P. Murani, and G. H. Lander, J. Magn. Magn. Mater 15-18, 973 (1980).
- <sup>8</sup>C. Stassis, H. W. Deckman, B. M. Harmon, J. P. Desclaux, and A. J. Freeman, Phys. Rev. B 15, 369 (1977).
- <sup>9</sup>W. Marshall and R. D. Lowde, Rep. Prog. Phys. 31, 705 (1968).
- <sup>10</sup>T. Moriya, J. Phys. Soc. Jpn. 18, 516 (1963).
- <sup>11</sup>K. W. Becker, P. Fulde, and J. Keller, Z. Phys. B 28, 9 (1977).
- <sup>12</sup>K. Pierre, A. P. Murani, and R. M. Gelera, J. Phys. F 11, 679 (1981).
- <sup>13</sup>E. Holland-Moritz, D. Wohlleben, and M. Loewenhaupt, Phys. Rev. B 25, 7482 (1982).
- <sup>14</sup>B. H. Grier, R. D. Parks, S. M. Shapiro, and C. F. Majkrzak, Phys. Rev. B 24, 6242 (1981); T. M. Holden, W. J. L. Buyers, P. Martel, M. B. Maple, and M. Trovar, in *Valence Instabilities*, edited by P. Wachter and H. Boppart (North-Holland, Amsterdam, 1982), p. 325.
- <sup>15</sup>A. P. Murani, Phys. Rev. B 28, 2308 (1983); J. Phys. C 33, 6359 (1983).